Photochemical C−H Bond Activation Reactivity of $(HBPz'_3)Rh(CO)_2$ (Pz′ = 3,5-Dimethylpyrazolyl) in Alkane Solutions

Agus A. Purwoko and Alistair J. Lees*

Department of Chemistry, Binghamton University, State University of New York, Binghamton, New York 13902-6016

Received September 15, 1995[⊗]

The intermolecular C−H bond activation photochemistry of $(HBPz'_3)Rh(CO)_2$ (Pz′ = 3,5-dimethylpyrazolyl) has been investigated in various alkane solutions at 293 K. Excitations have been performed at 313−458 nm into the lowest energy absorption band of this complex, and the reactions have been monitored throughout photolysis by *in situ* UV−visible and FTIR spectroscopy. The spectral results reveal that the photochemistry is exceptionally clean and that the reagent complex can be completely converted to the corresponding $(HBPz'_3)Rh(CO)(R)H$ photoproduct at each of the irradiation wavelengths. Absolute photochemical quantum efficiencies (ϕ_{CH}) for these reactions have been determined and illustrate that the intermolecular C−H bond activation process is strongly wavelength dependent. Very effective conversion ($\phi_{CH} = 0.31-0.34$) is attained upon near-UV excitation at 313 or 366 nm. In contrast, inefficient conversion ($\phi_{CH} = 0.010-0.011$) is observed on visible excitation at 458 nm. The differences in reactivities are interpreted on a photophysical scheme in which the irradiations produce two ligand field (LF) electronically excited states with different primary photoproducts. The thermal chemistry of $(HBPz'_3)Rh(CO)_2$ in room-temperature solution is characterized as involving facile $\eta^3 \leftrightarrow \eta^2$ ligand interconversions. Accordingly, the complex is readily protonated to form $[\{\eta^2\text{-}HBPz'_2(Pz'H)\}Rh(CO)_2]BF_4$, and when PPh_3 is added to a solution of $(HBPz'_3)Rh(CO)_2$, the ligand substitution product, $(HBPz'_3)Rh(CO)PPh_3$, is formed immediately. In contrast, there is no evidence of thermal ligand scavenging of $(HBPz'_3)Rh(CO)_2$ by pyridine and upon irradiation in pyridine solutions the photochemistry is dominated by the C−H activation reaction of the hydrocarbon solvent. In triethylsilane solutions the observed spectral changes reveal that intermolecular Si−H bond activation takes place readily on excitation of $(HBPz'_3)Rh(CO)_2$ at 366 nm. The thermal chemistry of the analogous square planar complex $(H_2BPz_2)Rh(CO)_2$ has been investigated, and the complex has been found to be reactive toward PPh_3 and not R−H in room-temperature solution under dark conditions. These experimental observations imply that the long-wavelength (458 nm) photochemistry and thermal chemistry of $(HBPz'_3)Rh(CO)_2$ are associated with a $(\eta^2\text{-}HBPz'_3)Rh(CO)_2$ intermediate that is unable to facilitate hydrocarbon C−H bond activation. Importantly, the observed results also suggest that the short-wavelength (313, 366 nm) photochemistry proceeds via an extremely short-lived monocarbonyl $(HBPz'_3)Rh(CO)$ complex that undergoes efficient C−H activation.

Introduction

Over the past several years, much attention has been paid to the nature of the photochemical mechanisms whereby transition-metal organometallic complexes facilitate intermolecular C−H bond activation reactions in hydrocarbon solutions.[1] In a number of systems, the identity of key reaction intermediates has been determined. Upon photochemical excitation of $(\eta^5\text{-}C_5R_5)ML_2$ and $(\eta^5\text{-}C_5R_5)ML(H)_2$ (R = H, Me; M = Rh, Ir; L = olefin, PR_3, CO), it has been established that the intermolecular C−H activation stems from an unsaturated 16-electron $(\eta^5\text{-}C_5R_5)ML$ primary photoproduct that rapidly forms a solvent-adduct complex, $(\eta^5\text{-}C_5R_5)ML\cdots S$, in even normally inert solvents (S), before reacting with R−H bonds. Following initial synthetic and competitive rate investigations,[2−4] various experimental techniques have been employed to elucidate the mechanisms of these C−H activation reactions; these have involved matrix isolation,[5,6] solvation in liquefied rare gases,[7] steady-state photolysis,[8] and laser-flash photolysis.[9] The rates of alkane C−H bond activation to $(\eta^5\text{-}C_5H_5)Rh(CO)_2$ in the gas

[⊗] Abstract published in *Advance ACS Abstracts,* January 1, 1996.

(1) Crabtree, R. H. *The Organometallic Chemistry of the Transition Metals*, 2nd Ed.; Wiley-Interscience: New York, 1994; p 321.
(2) (a) Janowicz, A. H.; Bergman, R. G. *J. Am. Chem. Soc.* **1982**, *104*, 352; **1983**, *105*, 3929. (b) Periana, R. A.; Bergman, R. G. *Organometallics* **1984**, *3*, 508. (c) Wax, M. J.; Stryker, J. M.; Buchanan, J. M.; Kovac, C. A.; Bergman, R. G. *J. Am. Chem. Soc.* **1984**, *106*, 1211. (d) Janowicz, A. H.; Periana, R. A.; Buchanan, J. M.; Kovak, C. A.; Stryker, J. M.; Wax, M. J.; Bergman, R. G. *Pure Appl. Chem.* **1984**, *56*, 13. (e) Periana, R. A.; Bergman, R. G. *J. Am. Chem. Soc.* **1984**, *106*, 7272.
(3) (a) Hoyano, J. K.; Graham, W. A. G. *J. Am. Chem. Soc.* **1982**, *104*, 3723. (b) Hoyano, J. K.; McMaster, A. D.; Graham, W. A. G. *J. Am. Chem. Soc.* **1983**, *105*, 7190.
(4) Jones, W. D.; Feher, F. J. *J. Am. Chem. Soc.* **1982**, *104*, 4240; **1984**, *106*, 1650; **1985**, *107*, 620; *Organometallics* **1983**, *2*, 562; **1983**, 2, 686; *Inorg. Chem.* **1984**, *23*, 2376.
(5) (a) Rest, A. J.; Whitwell, I.; Graham, W. A. G.; Hoyano, J. K.; McMaster, A. D. *J. Chem. Soc., Chem. Commun.* **1984**, 624; *J. Chem. Soc., Dalton Trans.* **1987**, 1181. (b) Bloyce, P. E.; Rest, A. J.; Whitwell, I.; Graham, W. A. G.; Holmes-Smith, R. *J. Chem. Soc., Chem. Commun.* **1988**, 846.
(6) (a) Haddleton, D. M.; Perutz, R. N. *J. Chem. Soc., Chem. Commun.* **1985**, 1372. (b) Haddleton, D. M. *J. Organomet. Chem.* **1986**, *311*, C21. (c) Haddleton, D. M.; McCramley, A.; Perutz, R. N. *J. Am. Chem. Soc.* **1988**, *110*, 1810.
(7) (a) Haddleton, D. M.; Perutz, R. N.; Jackson, S. A.; Upmacis, R. K.; Poliakoff, M. *J. Organomet. Chem.* **1986**, *311*, C15. (b) Sponsler, M. B.; Weiller, B. H.; Stoutland, P. O.; Bergman, R. G. *J. Am. Chem. Soc.* **1989**, *111*, 6841. (c) Weiller, B. H.; Wasserman, E. P.; Bergman, R. G.; Moore, C. B.; Pimentel, G. C. *J. Am. Chem. Soc.* **1989**, *111*, 8288. (d) Weiller, B. H.; Wasserman, E. P.; Moore, C. B.; Bergman, R. G. *J. Am. Chem. Soc.* **1993**, *115*, 4326.
(8) (a) Drolet, D. P.; Lees, A. J. *J. Am. Chem. Soc.* **1990**, *112*, 5878; **1992**, *114*, 4186. (b) Purwoko, A. A.; Lees, A. J. *Coord. Chem. Rev.* **1994**, *132*, 155; *J. Organomet. Chem.* **1995**, *504*, 107.
(9) (a) Belt, S. T.; Haddleton, D. M.; Perutz, R. N.; Smith, B. P. H.; Dixon, A. J. *J. Chem. Soc., Chem. Commun.* **1987**, 1347. (b) Belt, S. T.; Grevels, F.-W.; Koltzbücher, W. E.; McCamley, A.; Perutz, R. N. *J. Am. Chem. Soc.* **1989**, *111*, 8373.

0020-1669/96/1335-0675$12.00/0

phase[10] and to (η^5-C_5Me_5)Rh(CO)X (X = Kr, Xe) in liquefied noble gas solvents at low temperature[11] have also been reported. Furthermore, theoretical models considering C−H bond activation of CH_4 lend support to a mechanism involving a coordinatively-unsaturated primary photoproduct arising from ligand dissociation.[12]

In recent photolysis studies of (η^5-C_5H_5)Rh(CO)$_2$ and (η^5-C_5Me_5)Rh(CO)$_2$ absolute photochemical quantum efficiencies (ϕ_{CH}) were determined for the intermolecular C−H activation processes in solution.[8] Even though the alkyl hydrido products are themselves photochemically unstable, it was possible to record ϕ_{CH} following a kinetic analysis of spectral data under conditions where photosubstitution and C−H/Si−H activation readily take place. From these ϕ_{CH} results it was shown that activation of C−H and Si−H bonds proceeds by a dissociative mechanism involving CO extrusion, whereas photosubstitution takes place via another mechanism involving competitive ligand scavenging for an unsaturated metal center. The latter process is believed to initially involve a ring slippage ($\eta^5 \rightarrow \eta^3$) rearrangement of the cyclopentadienyl ligand. Importantly, the photolysis studies have also shown that the solution photochemistry is strongly wavelength dependent and these mechanisms occur from two different electronically-excited states. Excitation of (η^5-C_5H_5)Rh(CO)$_2$ in the UV region (313 nm) results in efficient photochemical C−H reactivity ($\phi_{CH} \sim 0.2-0.4$), while excitation in the visible region (458 nm) leads to inefficient reaction ($\phi_{CH} \sim 0.002$).

Recently, we have begun to investigate the photochemistry of (HBPz′$_3$)Rh(CO)$_2$ (Pz′ = 3,5-dimethylpyrazolyl)[8b,13] following an earlier report[14] that C−H bond activation of saturated and aromatic hydrocarbons takes place readily in daylight at room temperature (see eq 1). Our preliminary results have

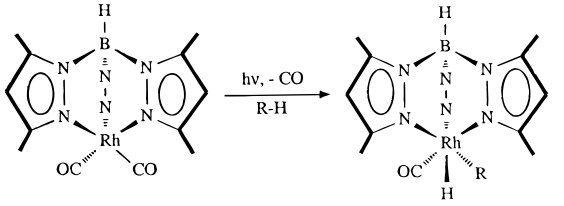

(1)

N–N = third pyrazolyl ring

indicated that this reaction can be taken to completion efficiently in alkane solutions and without interference from thermal processes or secondary photoreactions. Consequently, it is possible in this particular system to determine absolute quantum efficiencies for the C−H bond activation reaction, providing both an insight into the photochemical mechanism and quantitative data that will permit a useful comparison with the (η^5-C_5H_5)Rh(CO)$_2$ and (η^5-C_5Me_5)Rh(CO)$_2$ systems. The results of a full photolysis study of the C−H activation reaction in various alkane solutions, including the effects of different excitation wavelengths, are reported here. Additionally, the solution photochemistry and C−H bond activation properties of the closely-related square planar complex (H_2BPz_2)Rh(CO)$_2$ are investigated to draw a comparison with the tris(pyrazolyl)-borate system.

Experimental Section

Materials. The chlorodicarbonylrhodium(I) dimer was obtained in high purity (>99%) from Strem Chemicals, Inc., and used as received. Potassium hydrotris(3,5-dimethylpyrazol-l-yl)borate, potassium dihydrobis(pyrazol-l-yl)borate, and 3,5-dimethylpyrazole were purchased from Aldrich Chemical Co. in high purity (97%) and used without further purification. Solvents used in syntheses were obtained as reagent grade from Fisher Scientific Co. and were dried over anhydrous calcium sulfate (Aldrich Chemical Co.) prior to use. The *n*-pentane used in the photoreactivity measurements was purchased from Fisher Scientific Co. as spectroscopic grade; isooctane, *n*-hexane, and *n*-heptane were obtained from Aldrich Chemical Co. as spectroscopic grade. Toluene (Baker Chemical Co.) was further purified by acid washing with concentrated H_2SO_4, dried over $LiAlH_4$, and then distilled under N_2 prior to use. *Caution*! This solvent was kept cool (below 30 °C) while acid washing. Neutral alumina chromatographic adsorbant (80−200 mesh) was obtained from Fisher Chemical Co. The triphenylphosphine and pyridine ligands were purchased from Aldrich Chemical Co. in high purity (97−99%); the latter was distilled prior to use. Triethylsilane was obtained from Aldrich Chemical Co. in high purity (99%) and was refluxed over 5 Å molecular sieves (Fisher Scientific Co.) for 4 h and subsequently distilled under a nitrogen atmosphere immediately prior to use. Hydrogen and nitrogen gases were obtained from the Linde Gas Division at Union Carbide in high purity (>99%). Nitrogen gas used for solvent deoxygenation was purchased as high research grade (>99.99% purity) and was itself deoxygenated and dried by passage over calcium sulfate (W. A. Hammond Co.), phosphorus pentoxide (Aldrich Chemical Co.), and a pelletized copper catalyst (BASF R3-11, Chemical Dynamics Co.) that had been activated with hydrogen gas, according to a previously described procedure.[15] Carbon monoxide was obtained from the Linde Gas Division of Union Carbide as CP grade (99.5% purity) and was further purified by passage through a 1-m tube (2-cm diameter) containing the above copper catalyst and then a 25-cm tube (4-cm diameter) containing a mixture of calcium sulfate and 5 Å molecular sieves.

Syntheses. The (HBPz′$_3$)Rh(CO)$_2$ complex was prepared via reaction of the chlorodicarbonylrhodium(I) dimer with potassium hydrotris(3,5-dimethylpyrazolyl)borate according to a procedure described by Ghosh.[14c] A suspension of K[HBPz′$_3$] (2.38 mmol) was formed by stirring in toluene (70 mL) for 15 min, and then [Rh(CO)$_2$Cl]$_2$ (1.03 mmol) was added. The reaction mixture was stirred in the dark for 2.5 h at room temperature and then filtered to remove KCl and any other unreacted materials. Subsequently, the filtrate was cooled to −20 °C for 24 h to form an orange-yellow solid, which was dried *in vacuo*. The supernatant fluid was concentrated to approximately half the original volume and cooled to −20 °C for a further 48 h, giving additional solid product. IR for (HBPz′$_3$)Rh(CO)$_2$ in *n*-pentane: ν(CO) 2054, 1980 cm^{-1} (lit.[14a] in *n*-hexane: ν(CO) 2054, 1981 cm^{-1}). Mp: 205 °C dec.

The [{η^2-HBPz′$_2$(Pz′H)}Rh(CO)$_2$]BF$_4$ complex was prepared by the addition of tetrafluoroboric acid (5 mmol) to (HBPz′$_3$)Rh(CO)$_2$ (0.12 mmol) in CH_2Cl_2 (20 mL) under stirring.[16] This reaction was carried out in the dark. After 1 min FTIR spectra were acquired from the resultant light-yellow solution. IR for [{η^2-HBPz′$_2$(Pz′H)}Rh(CO)$_2$]BF$_4$ in CH_2Cl_2: ν(CO) 2090, 2026 cm^{-1} (lit.[16] in CH_2Cl_2: ν(CO) 2091, 2026 cm^{-1}).

The (HBPz′$_3$)Rh(CO)PPh$_3$ derivative was synthesized by adding PPh_3 (0.4 mmol) to a stirred deoxygenated solution of (HBPz′$_3$)Rh(CO)$_2$ (0.4 mmol) in *n*-pentane under dark conditions. After 30 min the mixture was analyzed by UV−visible and FTIR spectroscopy. UV−visible for (HBPz′$_3$)Rh(CO)PPh$_3$ in *n*-pentane: 359 nm (λ_{max}). IR for (HBPz′$_3$)-Rh(CO)PPh$_3$ in *n*-pentane: ν(CO) 1981 cm^{-1}. The solution was subsequently filtered and the solvent evaporated *in vacuo* to yield a

(10) Wasserman, E. P.; Moore, C. B.; Bergman, R. G. *Science* **1992**, *255*, 315.
(11) (a) Schultz, R. H.; Bengali, A. A.; Tauber, M. J.; Weiller, B. H.; Wasserman, E. P.; Kyle, K. R.; Moore, C. B.; Bergman, R. G. *J. Am. Chem. Soc.* **1994**, *116*, 7369. (b) Bengali, A. A.; Schultz, R. H.; Moore, C. B.; Bergman, R. G. *J. Am. Chem. Soc.* **1994**, *116*, 9585.
(12) (a) Saillard, J.-Y.; Hoffman, R. *J. Am. Chem. Soc.* **1984**, *106*, 2006. (b) Ziegler, T.; Tschinke, V.; Fan, L.; Becke, A. D. *J. Am. Chem. Soc.* **1989**, *111*, 9177.
(13) Purwoko, A. A.; Lees, A. J. *Inorg. Chem.* **1995**, *34*, 424.
(14) (a) Ghosh, C. K.; Graham, W. A. G. *J. Am. Chem. Soc.* **1987**, *109*, 4726. (b) Bloyce, P. E.; Mascetti, J.; Rest, A. J. *J. Organomet. Chem.* **1993**, *444*, 223. (c) Ghosh, C. K. Ph.D. Dissertation, University of Alberta, Edmonton, Alberta, Canada, 1988.
(15) Schadt, M. J.; Gresalfi, N. J.; Lees, A. J. *Inorg. Chem.* **1985**, *24*, 2492.
(16) Ball, R. G.; Ghosh, C. K.; Hoyano, J. K.; McMaster, A. D.; Graham, W. A. G. *J. Chem. Soc., Chem. Commun.* **1989**, 341.

light-yellow solid. This product was especially prone to decomposition, and further spectroscopic measurements were not obtained.

The $(HBPz'_3)Rh(CO)(SiEt_3)H$ complex was prepared by 366-nm photolysis of $(HBPz'_3)Rh(CO)_2$ (0.5 mmol) in Et_3SiH (10 mL) using a medium-pressure 200-W mercury arc lamp with an interference filter to isolate the excitation wavelength. The reaction was performed under a N_2 atmosphere and with continuous stirring. FTIR spectra taken during the irradiation indicated that the reaction was essentially complete after 20 min; following solvent removal, a light-yellow solid was obtained. UV−visible for $(HBPz'_3)Rh(CO)(SiEt_3)H$ in *n*-pentane: 283 nm (λ_{max}). IR for $(HBPz'_3)Rh(CO)(SiEt_3)H$ in *n*-pentane: ν(RhH) 2086 cm^{-1}, ν(CO) 2020 cm^{-1}.

The $(H_2BPz_2)Rh(CO)_2$ complex was synthesized according to literature methods[17] with minor modifications. A suspension of $K[H_2BPz_2]$ (1.88 mmol) in toluene (40 mL) was stirred for 15 min under a N_2 atmosphere, and then $[Rh(CO)_2Cl]_2$ (0.96 mmol) was added. A black precipitate formed immediately, which was filtered off and dried *in vacuo*. The product was sublimed at room temperature to yield a bright yellow solid. IR for $(H_2BPz_2)Rh(CO)_2$ in *n*-pentane: ν(CO) 2084, 2020 (lit.[17a] in hexane: ν(CO) 2088, 2022 cm^{-1}).

The $(H_2BPz_2)Rh(CO)PPh_3$ derivative was obtained by addition of PPh_3 (0.35 mmol) to $(H_2BPz_2)Rh(CO)_2$ (0.20 mmol) in CH_2Cl_2 with stirring. The resultant yellow solution was further stirred for 5 min followed by solvent evaporation and drying *in vacuo* to yield a yellow product. UV−visible for $(H_2BPz_2)Rh(CO)PPh_3$ in CH_2Cl_2: 357 nm (λ_{max}). IR for $(H_2BPz_2)Rh(CO)PPh_3$ in CH_2Cl_2: ν(CO) 1991 cm^{-1} (lit.[17b] in Nujol: ν(CO) 1969 cm^{-1}).

Equipment and Procedures. UV−visible spectra were recorded on a Hewlett-Packard Model 8450A diode-array spectrometer. Spectra were obtained from solutions held in regular 1-cm quartz cuvettes, and the reported band maxima are considered accurate to ±2 nm. Infrared spectra were recorded on a Nicolet Model 20SXC Fourier transform infrared (FTIR) spectrometer. Spectra were obtained from solutions using a NaCl cell of 1-mm path length, and the reported band maxima are considered accurate to ±0.5 cm^{-1}.

Visible photolyses at 458 nm were performed with a Lexel Corp. Model 95-4 4-W argon ion laser; the incident laser light intensity was calibrated by means of a Lexel Corp. Model 504 external power meter. Typically, laser powers of 30−60 mW (6.9×10^{-6} to 1.4×10^{-5} einstein min^{-1}) were employed for these 458-nm irradiations, although results were also obtained with reduced laser light powers between 10 and 20 mW and the determined quantum efficiency values were the same. UV photolyses at 313, 366, and 405 nm were carried out with light from an Ealing Corp. medium-pressure 200-W mercury arc lamp and housing apparatus set on an optical rail. Bandpass interference filters (10 nm, Ealing Corp.) were used to isolate the excitation wavelength. The incident light intensities were determined by ferrioxalate[18] and Aberchrome 540 actinometry[19] and were typically in the range 5.2×10^{-7} to 1.1×10^{-6} einstein min^{-1}.

In all irradiation experiments, the solution temperatures were controlled to ±0.1 K between 273 and 303 K by circulating a thermostated ethylene glycol−water mixture through a jacketed cell holder. Solutions were stringently filtered through 0.22-μm Millipore filters and deoxygenated by purging with prepurified nitrogen gas for 15 min prior to light excitation. Solutions saturated with CO were prepared by initially bubbling CO gas through the solution for 30 min and then stirring the solution for a further 30 min under a sealed CO atmosphere. During photolysis, the solutions were rapidly stirred to ensure sample homogeneity and a uniform absorbance in the light path. UV−visible and FTIR spectra were obtained from solutions at regular intervals throughout irradiation; resultant quantum efficiency values were determined in triplicate and were found to be reproducible to within ±5% in each case. The C−H bond activation reactions were also measured in the dark to assess the extent of thermal processes, and these were determined to be negligible during the course of the photolysis experiments.

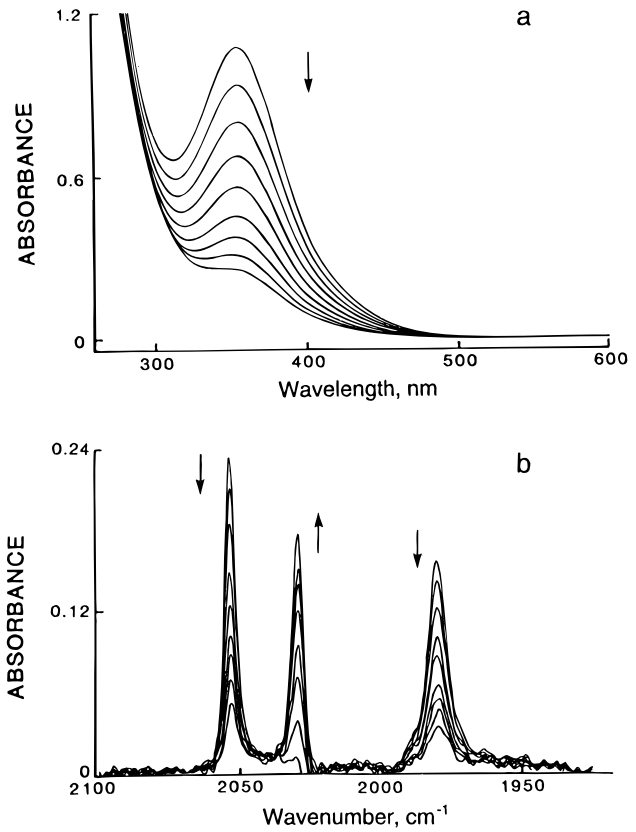

Figure 1. (a) UV−visible and (b) FTIR absorption spectral changes accompanying the 366-nm photolysis of $(HBPz'_3)Rh(CO)_2$ in deoxygenated *n*-pentane at 293 K. Spectra are depicted following 45 s irradiation time intervals; initial spectra were recorded prior to irradiation.

Results

Photolyses of $(HBPz'_3)Rh(CO)_2$ were carried out in several alkane solvents at room temperature, and in each case the photochemical C−H bond activation reaction was monitored by UV−visible and FTIR spectroscopy. Figure 1a illustrates the UV−visible absorption spectra recorded at 45 s time intervals during the 366-nm excitation of $(HBPz'_3)Rh(CO)_2$ in *n*-pentane; the lowest energy absorption band, centered at 356 nm (ϵ_{max} = 2100 M^{-1} cm^{-1}),[8b] progressively decreases in intensity as the reaction proceeds. Figure 1b depicts the FTIR absorption spectra accompanying the same photolysis experiment; the spectra reveal that there is a smooth conversion from the dicarbonyl complex (ν(CO) at 2054 and 1980 cm^{-1}) to the monocarbonyl hydrido photoproduct (ν(CO) at 2029 cm^{-1}, lit.[14c] 2031 cm^{-1}). These spectral results are entirely in accordance with the intermolecular C−H bond activation reaction (eq 2)

$$(HBPz'_3)Rh(CO)_2 \xrightarrow[C_5H_{12}]{h\nu} (HBPz'_3)Rh(CO)(C_5H_{11})H + CO \qquad (2)$$

reported by Ghosh and Graham.[14a,c] Moreover, the photochemistry here is especially clean, and complete conversions to the hydrido product were achieved at each of the excitation wavelengths used without any interference from secondary photoprocesses or side reactions. Indeed, spectra recorded from solutions that were kept in the dark at 293 K have shown that there are negligible contributions from thermal reactions during the course of these photochemical transformations.

(17) (a) King, R. B.; Bond, A. *J. Organomet. Chem.* **1974**, *73*, 115. (b) Bonati, F.; Minghetti, G.; Banditelli, G. *J. Organomet. Chem.* **1975**, *87*, 365.
(18) (a) Parker, C. A. *Proc. R. Soc. London, Ser. A* **1953**, *220*, 104. (b) Hatchard, C. G.; Parker, C. A. *Proc. R. Soc. London, Ser. A* **1956**, *235*, 518. (c) Calvert, J. G.; Pitts, J. N. *Photochemistry*; Wiley: New York, 1966.
(19) Heller, H. G.; Langan, J. N. *J. Chem. Soc., Perkin Trans.* **1981**, *341*.

Table 1. FTIR Absorption Spectra for $(HBPz'_3)Rh(CO)_2$ and Its C−H Bond Activation Photoproducts at 293 K

complex	solvent	ν(CO), cm^{-1}
$(HBPz'_3)Rh(CO)_2$	*n*-pentane	2054, 1980
$(HBPz'_3)Rh(CO)(C_5H_{11})H$	*n*-pentane	2029
$(HBPz'_3)Rh(CO)(C_6H_{13})H$	*n*-hexane	2029
$(HBPz'_3)Rh(CO)(C_7H_{15})H$	*n*-heptane	2028
$(HBPz'_3)Rh(CO)(C_8H_{17})H$	isooctane	2028

UV−visible and FTIR spectra were obtained following irradiation of $(HBPz'_3)Rh(CO)_2$ in several other alkane solvents at room temperature, and the results are very similar to those observed in *n*-pentane. In each solvent, the lowest energy absorption band of $(HBPz'_3)Rh(CO)_2$ is centered at 356 nm. For *n*-hexane and *n*-heptane the photolysis sequences indicate that there are complete conversions to the corresponding alkyl hydrido photoproducts at any of the excitation wavelengths employed. The spectral changes occurring in *n*-heptane have been previously described.[8b] For isooctane, though, a white precipitate was observed to form in the reaction cell following >30% conversion, illustrating that a secondary photoprocess takes place on prolonged excitation. In each case, the C−H activation photoproducts were not isolable but reacted immediately with added CCl_4 to form the $(HBPz'_3)Rh(CO)(R)Cl$ derivatives.[14a,c] Table 1 summarizes the FTIR spectral data recorded following photolyses of $(HBPz'_3)Rh(CO)_2$ in all the alkane solvents studied at 293 K.

Absolute photochemical quantum efficiencies (ϕ_{CH}) for intermolecular C−H bond activation were determined by monitoring the decline of the reactant's electronic absorption and infrared ν(CO) bands and application of eq 3. Here, C_R is

$$-dC_R/dt = \phi_{CH} I_0 (1 - 10^{-D}) \epsilon_R b C_R / D \qquad (3)$$

the concentration of the reactant $(HBPz'_3)Rh(CO)_2$ complex at varying photolysis times t, I_0 is the incident light intensity per unit solution volume, b is the cell path length, and D and ϵ_R are the optical density of the solution and molar absorptivity of the reactant complex at the irradiation wavelength, respectively. It should be noted that D is the total optical density of the solution and represents both of the absorbing species; the component $\epsilon_R b C_R/D$ is the fraction of the absorbed light that is absorbed by the reactant complex in the solution mixture. Consequently, eq 3 takes into account changing inner filter effects caused by the increasing light absorption of the photoproduct during the reaction. Rearrangement and integration of eq 3 yield

$$d \ln C_R = -\phi_{CH} I_0 \epsilon_R b [(1 - 10^{-D})/D] dt \qquad (4)$$

$$\ln(C_{t_i}/C_{t_0}) = \alpha \int_{t_0}^{t_i} [(1 - 10^{-D})/D]\, dt \qquad (5)$$

where

$$\alpha = -\phi_{CH} I_0 \epsilon_R b \qquad (6)$$

Plots of $\ln [(A_t - A_\infty)/(A_0 - A_\infty)]$ versus $\int_{t_0}^{t_i} [(1 - 10^{-D})/D]\, dt$, where A_0, A_t, and A_∞ are the infrared absorbance values of the reactant's ν(CO) bands throughout photolysis, were observed to yield straight lines of slope α to reaction completion, with $\alpha = -\phi_{CH} I_0 \epsilon_R b$; a typical plot is shown in Figure 2. The value α has units of reciprocal time, and the plots revealed linearity when $A_\infty = 0$. Coincident α values are obtained following kinetic analysis at either of the reactant's ν(CO) bands. Additionally, α values obtained on monitoring the increasing ν(CO) absorbance of the hydrido photoproduct were concordant in each case. These kinetic observations confirm the stoichiometric nature of the photochemical conversion. Finally, the determined ϕ_{CH} values were in all instances found to be unaffected by variations in the incident light intensity (see Experimental Section), indicating that the solution is homogeneous and, thus, has a uniform absorbance throughout the light path in each of these photochemical experiments.

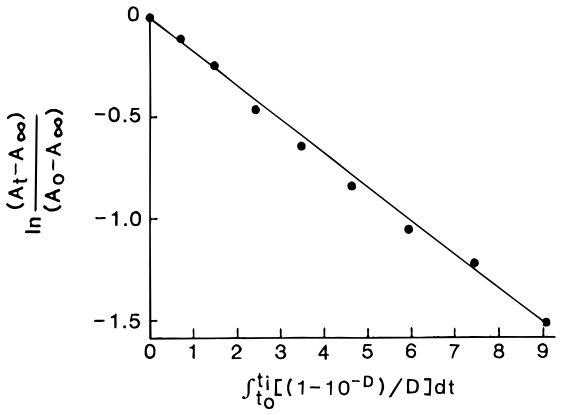

Figure 2. Kinetic representation of the decreasing FTIR absorbance at 2054 cm^{-1} (data taken from Figure 1).

Table 2. Absolute Photochemical Quantum Efficiencies (ϕ_{CH}) for Intermolecular C−H Bond Activation Reactions of $(HBPz'_3)Rh(CO)_2$ in Deoxygenated Alkane Solutions at 293 K

solvent	λ_{exc}, nm	ϕ_{CH}[a]	solvent	λ_{exc}, nm	ϕ_{CH}[a]
n-pentane	313	0.34	*n*-heptane	366	0.31
	366	0.32		458	0.010
	405	0.15	isooctane	366	0.31
	458	0.011		458	0.010
n-hexane	366	0.31			
	458	0.011			

[a] Values were determined in triplicate and were reproducible to within ±5%; data in *n*-heptane were taken from ref 8b.

Absolute photochemical quantum efficiencies (ϕ_{CH}) for the C−H bond activation reaction of $(HBPz'_3)Rh(CO)_2$ were recorded in several alkane solutions following excitation at various excitation wavelengths (see Table 2). Each excitation occurs into the lowest energy absorption feature of $(HBPz'_3)Rh(CO)_2$, and yet the ϕ_{CH} results are strongly dependent on the exciting wavelength. The oxidative addition reaction clearly proceeds very efficiently following excitation in the near-UV region (313, 366 nm), whereas this process is much less effective upon long-wavelength excitation (458 nm). Significantly, when the alkane solutions were presaturated with CO gas (ca. 9×10^{-3} M), there were no changes in the observed UV−visible and FTIR spectral progressions or in the resultant ϕ_{CH} data at any of the excitation wavelengths. Additionally, the ϕ_{CH} results in Table 2 reveal similar values for each of the alkane solvents at any of the particular excitation wavelengths.

Quantum efficiencies for the C−H bond activation reaction of $(HBPz'_3)Rh(CO)_2$ in *n*-pentane were determined at various temperatures. Following photolyses at 458 nm, the obtained ϕ_{CH} values are 0.0090 (273 K), 0.011 (283 K), 0.011 (293 K), and 0.012 (303 K). The least-squares line of an Arrhenius-type plot of $\ln \phi_{CH}$ versus $1/T$ yields an apparent activation energy, E_a, of 5.4 (±2.5) kJ mol^{-1}. Excitation at 366 nm results in ϕ_{CH} values of 0.28 (273 K), 0.30 (283 K), 0.32 (293 K), and 0.38 (303 K), yielding an apparent activation energy of 8.3 (±2.5) kJ mol^{-1}.

The infrared spectrum of $(HBPz'_3)Rh(CO)_2$ was recorded in CH_2Cl_2. At 293 K the FTIR spectrum exhibits two weak absorption features (ν(CO) at 2078 and 2009 cm^{-1}) which

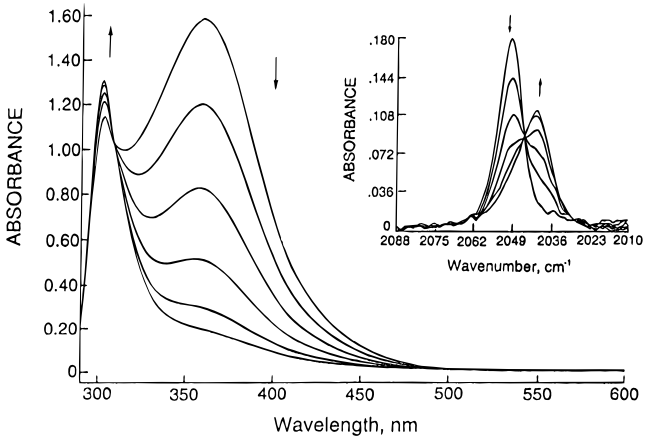

Figure 3. UV−visible absorption spectral changes accompanying the 366-nm photolysis of $(HBPz'_3)Rh(CO)_2$ in deoxygenated toluene containing 0.6 M py at 293 K. Spectra are depicted following 30 s irradiation time intervals; initial spectrum was recorded prior to irradiation. Inset illustrates FTIR absorption spectral changes recorded during the same experiment.

appear as high-energy shoulders to the main infrared absorption bands (ν(CO) at 2056 and 1981 cm^{-1}). In this connection, upon addition of excess $HBF_4{\cdot}OEt_2$ to the solution, the major infrared bands of the parent complex are shifted immediately to higher energy (ν(CO) at 2090 and 2026 cm^{-1}), representing the protonated $[\{\eta^2\text{-}HBPz'_2(Pz'H)\}Rh(CO)_2]BF_4$ complex.[16] This product was subsequently isolated (see Experimental Section).

Thermal and photochemical substitution reactions of $(HBPz'_3)Rh(CO)_2$ with triphenylphosphine (PPh_3) and pyridine (py) were investigated. The $(HBPz'_3)Rh(CO)_2$ complex was observed to react immediately in room-temperature *n*-pentane under dark conditions on addition of 0.1 M PPh_3 to form $(HBPz'_3)Rh(CO)PPh_3$ (ν(CO) at 1981 cm^{-1}), which was then characterized (see Experimental Section). The corresponding thermal reaction with py as the entering ligand was not observed when this solution was kept in the dark for several hours, permitting a study of the photochemistry. UV−visible and FTIR spectra recorded from 366-nm photolysis of $(HBPz'_3)Rh(CO)_2$ in deoxygenated toluene containing 0.6 M py at 293 K are shown in Figure 3. The spectra indicate that there is a smooth conversion to the hydrido photoproduct, $(HBPz'_3)Rh(CO)(C_7H_7)H$, with retention of sharp isosbestic points throughout the photolysis. FTIR data were not acquired below 2000 cm^{-1} because this region was masked by solvent absorption. The spectrum of the photoproduct was determined to be identical to that recorded following photolysis in toluene in the absence of added py (ν(CO) at 2042 cm^{-1}), and no evidence was obtained for the ligand photosubstitution product, $(HBPz'_3)Rh(CO)py$. Photolysis of $(HBPz'_3)Rh(CO)_2$ in neat py was found to result in decomposition of the parent complex, and there was no indication in the FTIR spectra for the growth of an oxidative addition product.

The photochemical intermolecular Si−H bond activation reaction of $(HBPz'_3)Rh(CO)_2$ was studied. Figure 4 depicts UV−visible and FTIR spectral sequences observed from the 366-nm photolysis of $(HBPz'_3)Rh(CO)_2$ in *n*-pentane containing 0.05 M Et_3SiH at room temperature. The UV−visible spectra show a decreasing absorption band, and the FTIR spectra illustrate a decline in the ν(CO) features of the parent complex at 2054 and 1980 cm^{-1} with a commensurate growth of ν(CO) bands at 2029 and 2020 cm^{-1}. The latter infrared absorptions are assigned to the C−H and Si−H activated products, respectively (see eqs 7 and 8). Both UV−visible and FTIR spectral data were obtained from the isolated silyl hydrido complex (see Experimental Section) and are consistent with the

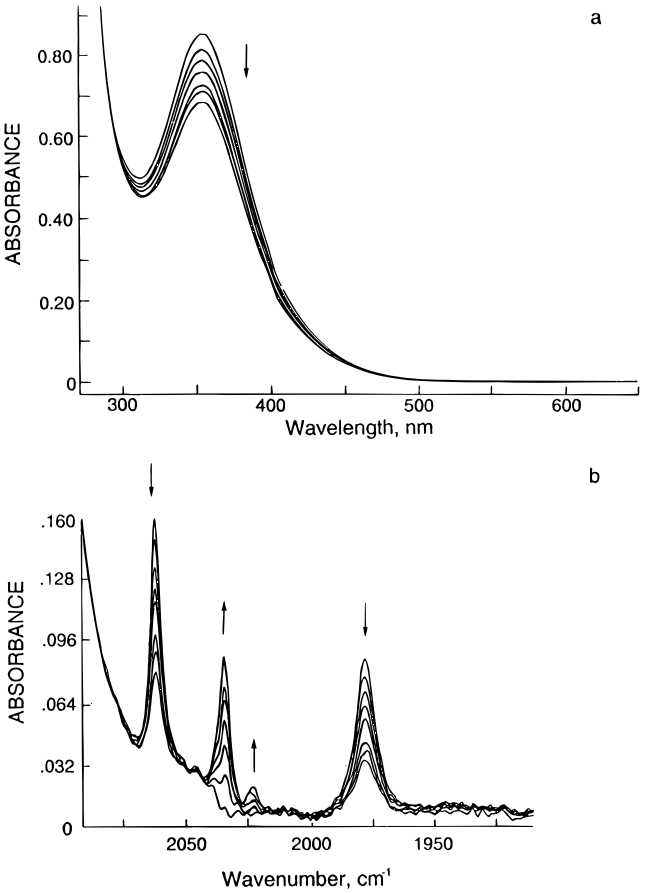

Figure 4. (a) UV−visible and (b) FTIR absorption spectral changes accompanying the 366-nm photolysis of $(HBPz'_3)Rh(CO)_2$ in deoxygenated *n*-pentane containing 0.05 M Et_3SiH at 293 K. Spectra are depicted following 2 min irradiation time intervals; initial spectra were recorded prior to irradiation.

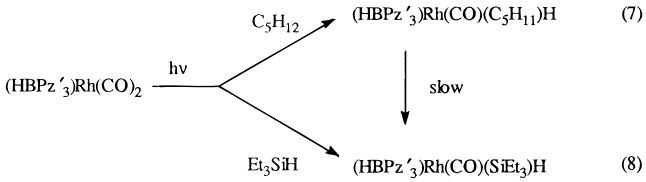

in situ photochemical observations. Further, it was noted that these two product bands grow simultaneously during irradiation and on subsequent monitoring of the photolyzed solution there were a further slow increase in the band at 2020 cm^{-1} and a decrease in the feature at 2029 cm^{-1}. The Si−H bond activation photochemistry was also carried out in neat Et_3SiH, and the observed spectral changes are analogous but more pronounced (see Figure 5). During irradiation, an infrared band (ν(CO) at 2020 cm^{-1}) was observed to appear, which represents the formation of the $(HBPz'_3)Rh(CO)(SiEt_3)H$ photoproduct. From a photokinetic analysis of these spectra, as described above, the quantum efficiency for Si−H bond activation (ϕ_{SiH}) at 366 nm was determined to be 0.16.

The closely-related square planar $(H_2BPz_2)Rh(CO)_2$ complex[17] was prepared (see Experimental Section) to provide a comparison of its thermal and photochemical properties. In fact, this compound was observed to be very stable in the absence of light in alkane solution at room temperature and there is no evidence for any significant degree of C−H activation. During 366-nm photolysis, however, the infrared bands of the complex (ν(CO) at 2084 and 2020 cm^{-1}) were seen to decrease but no new absorption bands were observed. Furthermore, an unidentified precipitate was observed to form as the light excitation

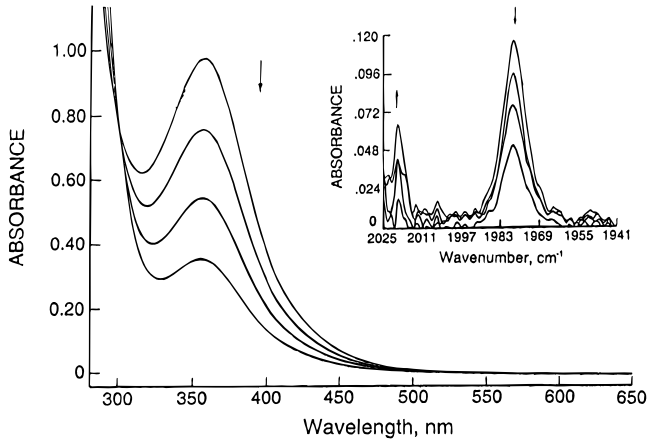

Figure 5. UV−visible absorption spectral changes accompanying the 366-nm photolysis of $(HBPz'_3)Rh(CO)_2$ in deoxygenated Et_3SiH at 293 K. Spectra are depicted following 2 min irradiation time intervals; initial spectrum was recorded prior to irradiation. Inset illustrates FTIR spectral changes recorded during the same experiment.

proceeded. Addition of 1 equiv of PPh_3 to $(H_2BPz_2)Rh(CO)_2$ in CH_2Cl_2 at room temperature yielded $(H_2BPz_2)Rh(CO)PPh_3$,[17b] which was subsequently isolated (see Experimental Section).

Discussion

Nature of the Electronically-Excited States. The observed C−H and Si−H bond activation reactions arise following irradiation at any of the employed wavelengths into the lowest energy absorption feature of $(HBPz'_3)Rh(CO)_2$. This band is understood to be ligand field (LF) in origin because its molar absorptivity is relatively low ($\epsilon_{max} = 2100\ M^{-1}\ cm^{-1}$)[8b] and the position of its energy maximum (356 nm) is insensitive to solvent changes. Moreover, it was recently determined that the $(HBPz'_3)Rh(CO)_2$ complex is not luminescent in 2-MeTHF and EPA solvent glasses or as a solid at 77 K,[8b,13] consistent with LF levels which are highly reactive and extremely short-lived.[20]

Photochemical C−H Bond Activation. The observed wavelength dependence of the photochemical quantum efficiency values (ϕ_{CH}) is unusual because each of the irradiations apparently involves excitation into the lowest energy absorption band (see Figure 1 and Table 2). Clearly, two electronically-excited states with different reactivities are being populated prior to the intermolecular C−H activation pathways. If only a single excited state was being produced, then the ϕ_{CH} data would be independent of excitation wavelength, recognizing that the determination of quantum efficiency accounts for variations in the light absorbance throughout the band envelope. Consequently, two different LF transitions are identified in the lowest energy absorption band of $(HBPz'_3)Rh(CO)_2$ (see Figure 1a). Indeed, the complex has a rather distinct absorption tail and irradiation at 458 nm in *n*-pentane at 293 K results in rather inefficient C−H activation ($\phi_{CH} = 0.011$), whereas excitation at 313 or 366 nm near the band maximum results in highly efficient C−H activation ($\phi_{CH} = 0.34$ and 0.32, respectively). Similar excitation wavelength dependencies are observed in the other hydrocarbon solvents (see Table 2).

To rationalize the different excited-state reactivities, it is important to first consider the thermal chemistry of this system. In room-temperature solution, the $(HBPz'_3)Rh(CO)_2$ complex exists as an equilibrium mixture of two isomers in which the tris(3,5-dimethylpyrazolyl)borate ligand undergoes facile tridentate (η^3) to bidentate (η^2) interconversions (see eq 9). The η^3 species is predominant at room temperature, and estimates

$$(\eta^3\text{-}HBPz'_3)Rh(CO)_2 \rightleftharpoons (\eta^2\text{-}HBPz'_3)Rh(CO)_2 \qquad (9)$$

of $\Delta G \approx 12.6$ kJ mol^{-1} and $K_{eq} \approx 0.01$ have been obtained for the equilibrium in CH_2Cl_2 at 298 K.[14c]

The rate of $\eta^3 \leftrightarrow \eta^2$ interconversion is apparently very rapid, as no evidence for the η^2 species has been obtained from ^1H NMR spectra of $(HBPz'_3)Rh(CO)_2$ in CD_2Cl_2, even at 183 K.[14c] Significantly, however, weak infrared features at 2078 and 2009 cm^{-1} are observed for the complex in CH_2Cl_2 at 298 K; these are assigned to the ν(CO) bands from $(\eta^2\text{-}HBPz'_3)Rh(CO)_2$ and are virtually isoenergetic with those of the square planar $(H_2BPz_2)Rh(CO)_2$ complex with ν(CO) bands at 2084 and 2020 cm^{-1}. Furthermore, the η^2 isomer has been isolated in the protonated form, $[\{\eta^2\text{-}HBPz'_2(Pz'H)\}Rh(CO)_2]BF_4$, following addition of HBF_4·OEt to a CH_2Cl_2 solution of $(HBPz'_3)Rh(CO)_2$. The ν(CO) bands of this protonated η^2 complex appear at 2090 and 2026 cm^{-1}, again similar in energy to those of the η^2 species. The crystal structure of this salt has been previously determined.[16]

Importantly, despite the extremely facile $\eta^3 \leftrightarrow \eta^2$ interconversion mechanism, it was found that no C−H bond activation chemistry took place in the dark from $(HBPz'_3)Rh(CO)_2$ over the time scale of these photochemical experiments. This eliminates the simple ligand $\eta^3 \leftrightarrow \eta^2$ dechelation process as being the key step in the C−H activation photochemistry. On the other hand, the η^2 species, because it is unable to oxidatively add to RH, is invoked in the reduced C−H activation reactivity from the lower energy LF state produced on long-wavelength photolysis. Although 458-nm excitation is expected to result in an effective $\eta^3 \rightarrow \eta^2$ ligand dechelation process, the subsequent $\eta^2 \rightarrow \eta^3$ back-reaction is obviously so facile that the net result is just a return to the parent $(HBPz'_3)Rh(CO)_2$ complex. In sharp contrast, the ϕ_{CH} data at 313 and 366 nm illustrate that excitation into the upper energy LF state results in highly effective C−H bond activation, clearly implying an entirely different reaction intermediate. Numerous ultrafast studies have now been performed for metal carbonyl complexes, and it is well established that CO dissociation reactions take place readily in this wavelength region.[21] Thus, an unsaturated monocarbonyl $(HBPz'_3)Rh(CO)$ complex is implicated, analogous to the primary photoproduct of the corresponding C−H activating $(\eta^5\text{-}C_5H_5)Rh(CO)_2$ and $(\eta^5\text{-}C_5Me_5)Rh(CO)_2$ systems.[5−11] Moreover, the lack of an observable dependence of ϕ_{CH} with added CO is completely consistent with extremely fast formation of a monocarbonyl photoproduced intermediate from a dissociative LF excited state. Subsequently, the intermediate will react rapidly with the hydrocarbon substrate (8.7 M *n*-pentane) before CO (ca. 9×10^{-3} M) can coordinate.

Recently, the photochemistry of $(HBPz'_3)Rh(CO)_2$ was studied in Nujol mulls at 12 and 77 K and in methane matrices at 12 K.[14b] In each case, no evidence was found for the C−H bond activation reaction at low temperature, although this

(20) Lees, A. J. *Chem. Rev.* **1987**, *87*, 711.

(21) (a) Bonneau, R.; Kelly, J. M. *J. Am. Chem. Soc.* **1980**, *102*, 1220. (b) Lees, A. J.; Adamson, A. W. *Inorg. Chem.* **1981**, *20*, 4381. (c) Kelly, J. M.; Long, C.; Bonneau, R. *J. Phys. Chem.* **1983**, *87*, 3344. (d) Simon, J. D.; Xie, X. *J. Phys. Chem.* **1986**, *90*, 6751; **1987**, *91*, 5538; **1989**, *93*, 291. (e) Wang, L.; Zhu, X.; Spears, K. G. *J. Am. Chem. Soc.* **1988**, *110*, 8695. (f) Joly, A. G.; Nelson, K. A. *J. Phys. Chem.* **1989**, *93*, 2876. (g) Lee, M.; Harris, C. B. *J. Am. Chem. Soc.* **1989**, *111*, 8963. (h) Xie, X.; Simon, J. D. *J. Am. Chem. Soc.* **1990**, *112*, 1130. (i) Yu, S.-C.; Xu, X.; Lingle, R.; Hopkins, J. B. *J. Am. Chem. Soc.* **1990**, *112*, 3668. (j) O'Driscoll, E.; Simon, J. D. *J. Am. Chem. Soc.* **1990**, *112*, 6580. (k) Dougherty, T. P.; Heilweil, E. J. *J. Chem. Phys.* **1994**, *100*, 4006; *Chem. Phys. Lett.* **1994**, *227*, 19. (l) Grubbs, W. T.; Dougherty, T. P.; Heilweil, E. J. *Chem. Phys. Lett.* **1994**, *227*, 480. (m) Dougherty, T. P.; Grubbs, W. T.; Heilweil, E. J. *J. Phys. Chem.* **1994**, *98*, 9396. (n) Arrivo, S. M.; Dougherty, T. P.; Grubbs, W. T.; Heilweil, E. J. *Chem. Phys. Lett.* **1995**, *235*, 247.

process was observed on warming the mull to 298 K. Both CO loss and ligand dechelation products were determined in low yield at 12 K, suggesting that there is insufficient thermal energy at this low temperature to remove CO from the solvent and matrix cages and, thus, facilitate C−H activation.

It is notable that the ϕ_{CH} values of Table 2 are essentially the same, within experimental error, for each of the hydrocarbons studied at any particular excitation wavelength. As discussed previously, however, the kinetic reactivity of a C−H bond does not always depend on the thermodynamic stability of the M−C bond of the alkylhydridometal complex.[2−4,22] Instead, the quantum efficiencies for C−H bond activation are likely to be predominantly influenced by the photophysical behavior occurring prior to the formation of the primary photoproducts and, specifically, by the deactivation rates from the LF excited states (*vide infra*).

The $(HBPz'_3)Rh(CO)_2$ molecule is clearly able to facilitate C−H activation readily, even under photochemical conditions in solution where additional scavenging ligands are present. When 0.1 M PPh_3 is added to the solution, the product $(HBPz'_3)Rh(CO)PPh_3$ is observed immediately in the dark, consistent with the facile $\eta^3 \rightarrow \eta^2$ thermal process and rapid ligand coordination. However, with the addition of 0.6 M py, a weakly coordinating ligand, there is no significant extent of thermal ligand scavenging, and the photochemistry is still dominated by C−H activation of the hydrocarbon solvent (see Figure 3), which is present at a much higher concentration (9.4 M toluene).

Photochemical Si−H Bond Activation. In hydrocarbon solutions containing triethylsilane both Si−H and C−H activation reactions are observed to take place. Results obtained for a solution of Et_3SiH in *n*-pentane (see Figure 4) reveal that the Si−H bonds are effectively activated at 366 nm, considering that the Et_3SiH concentration (0.05 M) is much less than that of the hydrocarbon (8.7 M *n*-pentane). Clearly, the $(HBPz'_3)Rh(CO)(SiEt_3)H$ photoproduct is more thermodynamically stable than the $(HBPz'_3)Rh(CO)(C_5H_{11})H$ species, a conclusion that is supported by the isolation of the former complex.

Interestingly, in neat Et_3SiH solution, the quantum efficiency at 366 nm for Si−H bond activation ($\phi_{SiH} = 0.16$) is substantially lower than those for C−H bond activation in the hydrocarbon solutions ($\phi_{CH} = 0.31-0.32$). Again, it appears that the thermodynamic stability of the product is not the determining influence on the quantum efficiencies. It is initially, though, somewhat surprising that there are variations in these observed quantum efficiencies because in each case the reaction with substrate takes place completely. As noted above, the back-reaction of the primary photoproduct with CO is not a competitive process, so variations in ϕ_{CH} and ϕ_{SiH} cannot be attributed to kinetic differences in the reactivity of the substrate molecules. Instead, the data imply that variations in the photophysical rate processes must be influential. A comparison of the quantum efficiencies suggests that the upper LF excited state is able to decay more effectively in neat Et_3SiH solution and, hence, reduce the extent that these reactive primary photoproducts are formed.

Photochemistry of $(H_2BPz_2)Rh(CO)_2$. This bis(pyrazolyl)borate complex has been previously characterized to have a square planar geometry.[17] Consequently, it provides a most useful comparison to the intermediate $(\eta^2\text{-}HBPz'_3)Rh(CO)_2$ implicated in the thermal chemistry and long-wavelength photochemistry of $(HBPz'_3)Rh(CO)_2$. In this regard, it is significant that the $(H_2BPz_2)Rh(CO)_2$ complex does not facilitate C−H activation of hydrocarbons thermally and, indeed, it is very stable in solution under dark conditions. Moreover, on addition of PPh_3, the $(H_2BPz_2)Rh(CO)PPh_3$ ligand substitution product forms immediately, indicating that the square planar complex is receptive toward nucleophiles but not R−H bonds. These observations strongly support the conclusion that the $(\eta^2\text{-}HBPz'_3)Rh(CO)_2$ species is involved in the long-wavelength photochemistry and thermal chemistry of $(HBPz'_3)Rh(CO)_2$ and yet it is completely ineffective at facilitating C−H bond activation.

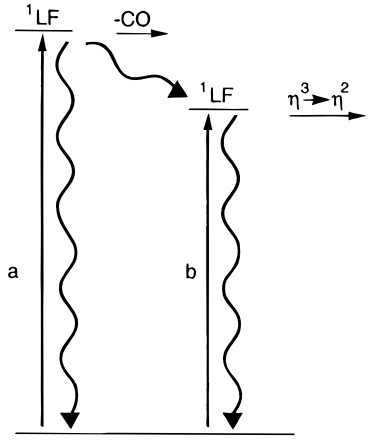

Figure 6. Photophysical representation of the lowest energy electronically-excited states and their deactivation pathways in $(HBPz'_3)Rh(CO)_2$ following (a) 366 and (b) 458 nm excitations.

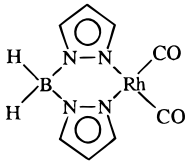

Photophysical Interpretation. A representation of the electronically-excited LF states and their deactivation processes is depicted in Figure 6. In this photophysical scheme, the excitation wavelength results are recognized by presenting different reactivities from two LF excited levels. The LF states are represented as singlets, although it is understood that a "pure" singlet designation is unrealistic in view of the high degree of spin−orbit coupling associated with this heavy metal complex.[20] On the basis of numerous studies of metal carbonyls, it can be anticipated that the radiationless and bond dissociative events occurring from these LF levels are extremely rapid and are essentially completed within a few picoseconds.[21] The primary photoproducts are, therefore, expected to be very short-lived and immediately form solvent (S) complexes, as postulated for $(\eta^5\text{-}C_5H_5)Rh(CO)\cdots S$ and $(\eta^5\text{-}C_5Me_5)Rh(CO)\cdots S$.[7−11] Indeed, in $(HBPz'_3)Rh(CO)_2$, all the photochemical results can be explained by similarly invoking $[(HBPz'_3)Rh(CO)]\cdots S$ and $[(\eta^2\text{-}HBPz'_3)Rh(CO)_2]\cdots S$ intermediates, as these species are subsequently able to undergo reaction to completion via R−H cleavage (C−H activation) or $\eta^2 \rightarrow \eta^3$ (ligand rechelation) processes, respectively.

In this interpretation, the quantum efficiencies for C−H activation will be predominantly determined by the primary photophysical processes. Consequently, it is perhaps then not surprising to find that the ϕ_{CH} values are so similar for $(HBPz'_3)Rh(CO)_2$ in the range of alkanes studied, because the radiationless deactivation rates from the LF excited states may be expected to be alike.[20,23] On the other hand, the ϕ_{SiH} value in Et_3SiH is lower than ϕ_{CH} in the hydrocarbons, suggesting that

(22) Jones, W. D.; Hessell, E. T. *J. Am. Chem. Soc.* **1993**, *115*, 554.

(23) Turro, N. J. *Modern Molecular Photochemistry*; University Science Books: Mill Valley, CA, 1991; p 174.

the nonradiative rates of decay from the upper ^{1}LF state proceed more rapidly in Et_3SiH. It is also worth pointing out that although the quantum efficiency values measured at 458 nm are considerably lower than those from higher energy excitations, they are not negligible for any of the hydrocarbons studied (see Table 2). This observation can be explained by understanding that the photochemical excitation at 458 nm does not populate the lowest energy excited state exclusively, as the long-wavelength absorption tail is not that distinct from the broad absorption envelope. Similarly, irradiation at 405 nm in *n*-pentane populates both LF levels and yields a ϕ_{CH} value that is of magnitude between those obtained from the 366 and 458 nm photolyses. Indeed, the wavelength dependence of ϕ_{CH} can be explained solely on the basis of two LF states that spectrally overlap and, although it is a reasonable interpretation to invoke nonradiative processes between them (because internal conversions are normally fast), it is not actually necessary to do so.

Finally, it should be noted that the temperature dependence of ϕ_{CH} following excitation at either 458 or 366 nm is small. At 458 nm this results in an apparent activation energy, E_a, of 5.4 ($\pm$2.5) kJ mol^{-1}. Similarly, at 366 nm the determined apparent activation energy, E_a, is 8.3 ($\pm$2.5) kJ mol^{-1}. These values are obviously much too low to be associated with thermal activation from the lower ^{1}LF state to the upper ^{1}LF level; an estimate of this energy gap based on the 366- and 458-nm excitations is 66 kJ mol^{-1}. Instead, it is more realistic to attribute the small E_a value for the photochemical C−H activation reaction to the bond dissociation step of R−H in $[(HBPz'_3)Rh(CO)]\cdots S$ (S = RH) to form $(HBPz'_3)Rh(CO)(R)H$.

Conclusions

The solution photochemistry of $(HBPz'_3)Rh(CO)_2$ is exceptionally clean and has enabled a quantitative characterization of the intermolecular C−H bond activation reaction in several hydrocarbon solvents at room temperature. The experimental results suggest a photophysical scheme in which two LF excited states give rise to entirely different photochemical reactivities. Associated studies of the thermal properties of $(HBPz'_3)Rh(CO)_2$ (and the closely-related $(H_2BPz_2)Rh(CO)_2$ complex) illustrate that the long-wavelength (458 nm) photochemistry is dominated by a $\eta^3 \rightarrow \eta^2$ ligand dechelation process, whereas the short-wavelength (313, 366 nm) photochemistry leads to efficient C−H activation via a rapid CO dissociation reaction.

Acknowledgment. We thank the Division of Chemical Sciences, Office of Basic Energy Services, Office of Energy Research, U.S. Department of Energy, for support of this research (Grant DE-FG02-89ER14039) and the Ministry of Education of the Republic of Indonesia for a graduate fellowship to A.A.P. We are grateful to Professor W. A. G. Graham (University of Alberta) for initially supplying a sample of $(HBPz'_3)Rh(CO)_2$ and to Stephen D. Tibensky for experimental assistance.

IC951199X